



# Unraveling beam self-healing

ANDREA AIELLO,<sup>1,2</sup> GIRISH S. AGARWAL,<sup>3,4</sup> MARTIN PAÚR,<sup>5</sup>  
BOHUMIL STOKLASA,<sup>5</sup> ZDENĚK HRADIL,<sup>5</sup> JAROSLAV ŘEHÁČEK,<sup>5</sup>  
PABLO DE LA HOZ,<sup>6</sup> GERD LEUCHS,<sup>1</sup> AND  
LUIS L. SÁNCHEZ-SOTO<sup>1,6,\*</sup>

<sup>1</sup>Max Planck Institut für die Physik des Lichts, Staudtstraße 2, 91058 Erlangen, Germany

<sup>2</sup>Institut für Theoretische Physik II, Friedrich-Alexander Universität Erlangen-Nürnberg, Staudtstraße 2, 91058 Erlangen, Germany

<sup>3</sup>Institute for Quantum Science and Engineering and Department of Biological and Agricultural Engineering, Texas A&M University, College Station, TX 77845, USA

<sup>4</sup>Department of Physics, Oklahoma State University, Stillwater, OK 74078, USA

<sup>5</sup>Department of Optics, Palacký University, 17. listopadu 12, 771 46 Olomouc, Czech Republic

<sup>6</sup>Departamento de Óptica, Facultad de Física, Universidad Complutense, 28040 Madrid, Spain

\*lsanchez@fis.ucm.es

**Abstract:** We show that, contrary to popular belief, diffraction-free beams not only may reconstruct themselves after hitting an opaque obstacle but also, for example, Gaussian beams. We unravel the mathematics and the physics underlying the self-reconstruction mechanism and we provide for a novel definition for the minimum reconstruction distance beyond geometric optics, which is in principle applicable to any optical beam that admits an angular spectrum representation. Moreover, we propose to quantify the self-reconstruction ability of a beam via a newly established degree of self-healing. This is defined via a comparison between the amplitudes, as opposite to intensities, of the original beam and the obstructed one. Such comparison is experimentally accomplished by tailoring an innovative experimental technique based upon Shack-Hartmann wave front reconstruction. We believe that these results can open new avenues in this field.

© 2017 Optical Society of America

**OCIS codes:** (050.1940) Diffraction; (070.7345) Wave propagation; (260.1960) Diffraction theory.

## References and links

1. Z. Bouchal, J. Wagner, M. Chlup, "Self-reconstruction of a distorted nondiffracting beam," *Opt. Commun.* **151**, 207–211 (1998).
2. M. V. Vasnetsov, I. G. Marienko, and M. S. Soskin, "Self-reconstruction of an optical vortex," *JETP Lett.* **71**, 130–133 (2000).
3. V. Garcés-Chávez, D. McGloin, M. D. Summers, A. Fernandez-Nieves, G. C. Splading, G. Cristobal, and K. Dholakia, "The reconstruction of optical angular momentum after distortion in amplitude, phase and polarization," *J. Opt. A: Pure Appl. Opt.* **6**, S235–S238 (2004).
4. J. Arlt, V. Garcés-Chávez, W. Sibbett, and K. Dholakia, "Optical micromanipulation using a Bessel light beam," *Opt. Commun.* **197**, 239–245 (2001).
5. V. Garcés-Chávez, D. McGloin, H. Melville, W. Sibbett, and K. Dholakia, "Simultaneous micromanipulation in multiple planes using a self-reconstructing light beam," *Nature* **419**, 145–147 (2002).
6. F. O. Fahrbach, P. Simon, and A. Rohrbach, "Microscopy with self-reconstructing beams," *Nat. Phot.* **4**, 780–785 (2010).
7. F. O. Fahrbach, and A. Rohrbach, "Propagation stability of self-reconstructing Bessel beams enables contrast-enhanced imaging in thick media," *Nat. Commun.* **3**, 632 (2012).
8. M. McLaren, T. Mhlanga, M. J. Padgett, F. S. Roux, and A. Forbes, "Self-healing of quantum entanglement after an obstruction," *Nat. Commun.* **5**, 3248 (2014).
9. J. Durmin, J. J. Miceli, Jr. and J. H. Eberly, "Diffraction-free beams," *Phys. Rev. Lett.* **58**, 1499–1501 (1987).
10. Z. Bouchal, "Resistance of nondiffracting vortex beams to amplitude and phase perturbations," *Opt. Commun.* **210**, 155–164 (2002).
11. S. H. Tao and X. Yuan, "Self-reconstruction property of fractional Bessel beams," *J. Opt. Soc. Am. A* **21**, 1192–1197 (2004).
12. P. Fischer, H. Little, R. L. Smith, C. Lopez-Mariscal, C. T. A. Brown, W. Sibbett and K. Dholakia, "Wavelength dependent propagation and reconstruction of white light Bessel beams," *J. Opt. A* **8**, 477–482 (2006).

13. X. Chu, "Analytical study on the self-healing property of Bessel beam," *Eur. Phys. J. D* **66**, 259 (2012).
14. J. Broky, G. A. Siviloglou, A. Dogariu, and D. N. Christodoulides, "Self-healing properties of optical Airy beams," *Opt. Express* **16**, 12880–12891 (2008).
15. M. Anguiano-Morales, A. Martínez, M. D. Iturbe-Castillo, S. Chávez-Cerda, and N. Alcalá-Ochoa, "Self-healing property of a caustic optical beam," *Appl. Opt.* **46**, 8284–8290 (2007).
16. P. Zhang, Y. Hu, T. Li, D. Cannan, X. Yin, R. Morandotti, Z. Chen, and X. Zhang, "Nonparaxial Mathieu and Weber accelerating beams," *Phys. Rev. Lett.* **109**, 193901 (2012).
17. V. Arrizón, D. Aguirre-Olivas, G. Mellado-Villaseñor, and S. Chávez-Cerda, "Self-healing in scaled propagation invariant beams," arXiv:1503.03125 (2015).
18. P. Vainty and R. P. Singh, "Self-healing property of optical ring lattice," *Opt. Lett.* **36**, 2994–2996 (2011).
19. J. D. Ring, J. Lindberg, A. Mourka, M. Mazilu, K. Dholakia, and M. R. Dennis, "Autofocusing and self-healing of Pearcey beams," *Opt. Express* **20**, 18955–18966 (2012).
20. S. Vyas, Y. Kozawa, and S. Sato, "Self-healing of tightly focused scalar and vector Bessel-Gauss beams at the focal plane," *J. Opt. Soc. Am. A* **28**, 837–843 (2011).
21. G. Wu, F. Wang, and Y. Cai, "Generation and self-healing of a radially polarized Bessel-Gauss beam," *Phys. Rev. A* **89**, 043807 (2014).
22. F. Wang, Y. Chen, X. Liu, Y. Cai, and S. A. Ponomarenko, "Self-reconstruction of partially coherent light beams scattered by opaque obstacles," *Opt. Express* **24**, 23735–23746 (2016).
23. A. Aiello, and G. S. Agarwal, "Wave-optics description of self-healing mechanism in Bessel beams," *Opt. Lett.* **39**, 6819–6822 (2014).
24. D. McGloin and K. Dholakia, "Bessel beams: Diffraction in a new light," *Contemp. Phys.* **46**, 15–28 (2005).
25. I. A. Litvin, M. G. McLaren, and A. Forbes, "A conical wave approach to calculating Bessel-Gauss beam reconstruction after complex obstacles," *Opt. Commun.* **282**, 1078–1082 (2009).
26. D. L. Andrews (Ed.), *Structured Light and Its Applications: An Introduction to Phase-Structured Beams and Nanoscale Optical Forces*, (Academic, 2008).
27. L. Mandel and E. Wolf, *Optical Coherence and Quantum Optics* (Cambridge University, 1995).
28. M. Born and E. Wolf, *Principles of Optics* (Cambridge University, 1999).
29. R. Kress, *Linear Integral Equations* (Springer, 1999).
30. K. Ball, "Ellipsoids of maximal volume in convex bodies," *Geom. Dedic.* **41**, 241–250 (1992).
31. M. A. Nielsen and I. L. Chuang, "Quantum Computation and Quantum Information," (Cambridge University, 2000).
32. X. Chu, and W. Wen, "Quantitative description of the self-healing ability of a beam," *Opt. Express* **22**, 6899–6904 (2012).
33. A. N. Kolmogorov and S. V. Fomin, *Elements of the Theory of Functions and Functional Analysis* (Dover, 1999).
34. M. Hillery, "Nonclassical distance in quantum optics," *Phys. Rev. A* **35**, 725–732 (1987).
35. V. Vedral, M. B. Plenio, M. A. Rippin, and P. L. Knight, "Quantifying entanglement," *Phys. Rev. Lett.* **78**, 2275–2278 (1997).
36. A. B. Klimov, L. L. Sánchez-Soto, E. C. Yustas, J. Söderholm, and G. Björk, "Distance-based degrees of polarization for a quantum field," *Phys. Rev. A* **72**, 033813 (2005).
37. S. Gnutzmann and K. Życzkowski, "Rényi–Wehrl entropies as measures of localization in phase space," *J. Phys. A* **34**, 10123 (2001).

## 1. Introduction

In recent years, the remarkable capacity of a beam to reconstruct itself after encountering an obstacle (frequently called self-healing) has attracted a good deal of attention [1–3] and has already found applications in diverse areas [4–8].

Self-healing has been long time considered as a distinctive feature of nondiffracting beams [9]; most prominently of Bessel beams [10–13], although also Airy [14], caustic [15], and Mathieu and Weber [16] beams have been examined.

It was subsequently realized that some diffracting beams, including the whole family of scaled propagation invariant beams [17] optical ring lattices [18], Pearcey beams [19], and tightly focused [20] and radially polarized [21] Bessel-Gauss beams, can self-reconstruct. However, there is still the widespread perception that the self-reconstruction hinges on engineering special beam profiles and, in many instances, it is sensitive to the obstruction size and shape, thereby limiting applications of this phenomenon [22].

Recently, a complete account of self-healing for Bessel beams has been given in terms of wave optics [23]. The basic mechanism can be entirely explained in terms of the propagation of plane waves with radial wave vectors lying on a ring. The results obtained are in agreement with the standard ones established from a geometrical approach [24, 25], yet they open a new

scope.

In this paper, still using a wave-optics methodology, we come to the conclusion that self-healing may occur, potentially, for almost any kind of beam. Note, though, that it is outside the scope of most self-healing researches, and the present work is not an exception, the study of self-reconstruction capabilities of structured optical beams, as multiple-beam assemblies and, more generally, beams with complex and intricate intensity, polarization, frequency and temporal structures [26].

Furthermore, we introduce an appropriate degree that quantifies the similarity between the field of the unperturbed beam (namely, the beam that would propagate as if the obstacle were not present) and the field of the perturbed one (that is, the beam that propagates behind the obstruction). In this way, we put in evidence that self-healing is a property of both the intensity and the phase of the spatial distribution of the beam. We experimentally test these issues with a Gaussian beam, whose intensity and phase are measured by means of a CCD camera and a Shack-Hartman wavefront sensor, finding an outstanding agreement with our theoretical predictions.

## 2. Self-healing as an eigenvalue problem

Let us first set the stage for our construction. We consider a scalar field  $\Psi(x, y, z)$  propagating along the  $z$ -axis. An obstruction, characterized by an amplitude transmission function  $t_O(x, y)$ , is placed in the plane  $z = 0$ . Here and hereafter with obstruction we denote any physical object that decreases the intensity of a light beam, possibly in a space-dependent manner, without changing directly phase and polarization of light. The amplitude  $\Psi_O(x, y, 0)$  of the obstructed field at the plane  $z = 0$  is

$$\Psi_O(x, y, 0) = t_O(x, y) \Psi(x, y, 0). \quad (1)$$

The angular spectrum representation [27] is probably the most germane method to deal with the field propagation. Accordingly, the amplitude  $\Psi_O(x, y, z)$  of the field transmitted at a distance  $z$  from the obstruction can be expressed as the plane-wave superposition

$$\Psi_O(x, y, z) = \frac{1}{(2\pi)^2} \iint_{-\infty}^{\infty} \exp(i\boldsymbol{\rho} \cdot \boldsymbol{\kappa}) \exp(izk_z) \left[ \iint_{-\infty}^{\infty} \widehat{t}_O(\boldsymbol{\kappa} - \boldsymbol{\kappa}') \widehat{\Psi}(\boldsymbol{\kappa}') d^2\boldsymbol{\kappa}' \right] d^2\boldsymbol{\kappa}. \quad (2)$$

The wide hat (not to be confused with the small hat marking unit vectors) will denote throughout the spatial Fourier transform of the corresponding function evaluated at  $z = 0$ ; i.e., its angular spectrum. Two-dimensional transverse vectors, in either real and Fourier space, are denoted with Greek letters:  $\boldsymbol{\rho} = x\hat{x} + y\hat{y}$  and  $\boldsymbol{\kappa} = k_x\hat{x} + k_y\hat{y}$ . In addition,  $k_z = (k^2 - \kappa^2)^{1/2}$ , with  $\kappa^2 = k_x^2 + k_y^2$ .

Given the function  $t_O(x, y)$ , one can always define the transmission function  $t_A(x, y)$  of an aperture complementary to the obstruction [28] via the Babinet principle  $t_A(x, y) + t_O(x, y) = 1$ . Therefore, (1) yields

$$\Psi_O(x, y, 0) = [1 - t_A(x, y)]\Psi(x, y, 0) \equiv \Psi(x, y, 0) - \Psi_A(x, y, 0). \quad (3)$$

Taking the absolute value squared of both sides of this equation and integrating over the whole  $xy$ -plane, we obtain

$$I[\Psi_O] = I[\Psi] + I[\Psi_A] - 2 \operatorname{Re} \iint_{-\infty}^{\infty} \Psi^*(x, y, 0) \Psi_A(x, y, 0) dx dy, \quad (4)$$

where  $I[h] = \iint_{-\infty}^{\infty} h^*(x, y, z) h(x, y, z) dx dy$  is the average beam intensity at the plane  $z$ .

Conventionally, a beam is dubbed self-healing when it has the ability to recover its amplitude or intensity profile after being obscured by an obstacle. Quite obviously, perfect self-reconstruction is impossible, even in principle, because, as Eq. (4) distinctly shows, the intensity of the transmitted field is unavoidably reduced unless  $\mathcal{I}[\Psi_A] = 0$ . We thus content ourselves with the condition

$$\Psi_O(x, y, z) \approx \lambda_0 \Psi(x, y, z), \quad \forall z \geq z_0, \quad (5)$$

where  $z_0$  denotes the so-called minimum reconstruction distance and the scaling factor  $\lambda_0 = \{\mathcal{I}[\Psi_O]/\mathcal{I}[\Psi]\}^{1/2}$  accounts for the average intensity reduction caused by the obstruction.

The left-hand side of (5) is given by (2), while the field in the right-hand side can be jotted down as

$$\Psi(x, y, z) = \frac{1}{2\pi} \iint_{-\infty}^{\infty} \exp(i\boldsymbol{\rho} \cdot \boldsymbol{\kappa}) \exp(izk_z) \widehat{\Psi}(\boldsymbol{\kappa}) d^2\boldsymbol{\kappa}. \quad (6)$$

Consequently, (5) can be equivalently recast as

$$\widehat{\Psi}_O(\boldsymbol{\kappa}) \approx \lambda_0 \widehat{\Psi}(\boldsymbol{\kappa}). \quad (7)$$

Notice carefully, though, that (7) does not contain the variable  $z$ , whereas the relation (5) is supposed to be valid only for  $z \geq z_0$ . The latter requirement cannot be ignored because (5) cannot be satisfied at  $z = 0$ , where instead (3) must be fulfilled. Of course, in (3) we are implicitly excluding the trivial case of a spatially-uniform semi-transparent intensity obstruction (think of, e.g., a neutral-density filter) such that  $\Psi_A(x, y, 0) = (1 - \lambda_0)\Psi(x, y, 0)$ .

Hence, we are apparently faced with a contradiction here. In fact, (7) constitutes more a statement about the obstruction rather than the field. This can be seen by rewriting (7) in the more enlightening form

$$\frac{1}{2\pi} \iint_{-\infty}^{\infty} \widehat{t}_O(\boldsymbol{\kappa} - \boldsymbol{\kappa}') \widehat{\Psi}(\boldsymbol{\kappa}') d^2\boldsymbol{\kappa}' \approx \lambda_0 \widehat{\Psi}(\boldsymbol{\kappa}). \quad (8)$$

With the equality sign, this is a homogeneous Fredholm integral equation [29] for the function  $\widehat{\Psi}(\boldsymbol{\kappa})$ , which has to be an eigenfunction with eigenvalue  $2\pi\lambda_0$ , of the integral kernel  $\widehat{t}_O(\boldsymbol{\kappa} - \boldsymbol{\kappa}')$  describing the obstruction. This means that the requirement (5) is indeed too much restrictive because it can be satisfied only by those beams whose angular spectrum (the eigenfunction) is unaffected by the interaction with the obstruction, apart from a trivial proportionality factor (the eigenvalue), as shown in (8).

### 3. Minimum reconstruction distance

Let us have a closer look at the minimum reconstruction distance  $z_0$ , after which a self-reconstructing beam is supposed to restore its profile. For a single plane wave  $\exp(i\mathbf{k} \cdot \mathbf{r})$ , with wave vector  $\mathbf{k} = k(\hat{x} \sin \theta \cos \phi + \hat{y} \sin \theta \sin \phi + \hat{z} \cos \theta)$ , this parameter can be straightforwardly estimated in the context of either geometrical and wave optics [23].

Actually, let us consider an arbitrary obstruction on the  $xy$ -plane with an area  $O$ . As sketched in Fig. 1, for a simply connected region  $O$ , we can always find the incircle (the largest circle inscribed in  $O$ ) and the excircle (the smallest circumscribed circle), both centered on the beam axis [30]. The respective radii are  $b$  (inradius) and  $a$  (exradius). Then, elementary considerations lead us to [24, 25]

$$z_0 \propto \frac{a}{\tan \theta}, \quad (9)$$

where the proportionality factor essentially depends on the shape of the obstruction.

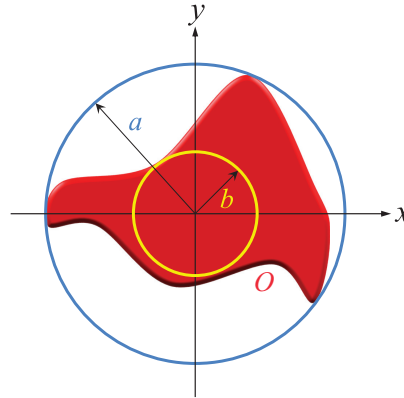


Fig. 1. Obstruction of area  $O$  represented in red. This region is circumscribed by the blue circle of radius  $a$  (extradius) and it inscribes the yellow circle of radius  $b$  (inradius). Both circles are centered along the  $z$ -axis of the beam at  $x = y = 0$ .

Next, notice that for our single plane wave

$$\frac{1}{\tan \theta} = \frac{k_z}{(k_x^2 + k_y^2)^{1/2}} = \frac{(k^2 - k_x^2 - k_y^2)^{1/2}}{(k_x^2 + k_y^2)^{1/2}}, \quad (10)$$

provided that  $k_x^2 + k_y^2 \leq k^2$ . This condition is necessary to maintain  $k_z$  real-valued and it limits the applicability of the equation above to beams whose angular spectrum does not contain evanescent waves [27]. We can thus regard  $z_0$  as a function of  $\kappa = (k_x^2 + k_y^2)^{1/2}$  in the  $k$ -space, namely

$$z_0 \sim a Z(\kappa) := a \frac{(k^2 - \kappa^2)^{1/2}}{\kappa}. \quad (11)$$

For an arbitrary beam, the transverse wave vector  $\boldsymbol{\kappa}$  has a density distribution function given by  $|\widehat{\Psi}(\boldsymbol{\kappa})|^2$ . So, we can define the minimum reconstruction distance  $z_0$  as the expected value of the function  $a Z(\kappa)$ ; namely,

$$\frac{z_0}{a} = \langle Z(\boldsymbol{\kappa}) \rangle = \frac{\iint \frac{(k^2 - \kappa^2)^{1/2}}{\kappa} |\widehat{\Psi}(\boldsymbol{\kappa})|^2 d^2 \boldsymbol{\kappa}}{\iint |\widehat{\Psi}(\boldsymbol{\kappa})|^2 d^2 \boldsymbol{\kappa}}, \quad (12)$$

where both integrals are limited to the disk  $k_x^2 + k_y^2 \leq k^2$ . We stress that this formula assigns a definite value of  $z_0$  to any density  $|\widehat{\Psi}(\boldsymbol{\kappa})|^2$ : self-healing does occur for any beam.

#### 4. Gaussian beams

As the Gaussian beam is the simplest example of a transversally unbounded diffracting beam, we shall use it as our thread to test the proposed concepts. We take it to be a Gaussian of waist  $w_0$ , so it can be written as

$$\Psi(x, y, z) = \exp(ikz)\psi(x, y, z), \quad (13)$$

with  $\psi(x, y, z)$  being the fundamental solution of the paraxial wave equation:

$$\psi(x, y, z) = \frac{1}{z - iz_R} \exp \left[ i \frac{k}{2} \left( \frac{x^2 + y^2}{z - iz_R} \right) \right], \quad (14)$$

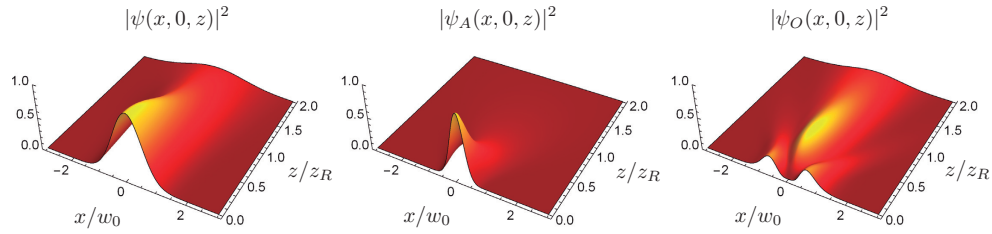


Fig. 2. Intensity distributions (evaluated at  $y = 0$ ), of (from left to right): the incident field  $\psi(x, 0, z)$ , the “virtual” field transmitted by the aperture complementary to the obstruction  $\psi_A(x, 0, z)$ , and the field transmitted behind the obstacle  $\psi_O(x, 0, z)$ . The plots correspond to a Gaussian beam  $w_0 = 0.26$  mm and a soft-edge Gaussian obstruction with full width  $a/w_0 = 0.28$ . At  $z/z_R = 2$ , the intensity profiles of  $\psi(x, 0, z)$  and  $\psi_O(x, 0, z)$  appear very similar.

and  $z_R = kw_0^2/2$  denotes the Rayleigh range.

To facilitate the calculations, the obstruction is taken as a soft-edge Gaussian obstacle of full width  $2a$  located along the axis of the beam at  $z = 0$ . This is described by the transmission function

$$t_O(x, y) = 1 - \exp\left(-\frac{|\boldsymbol{\rho} - \boldsymbol{\rho}_0|^2}{2a^2}\right), \quad (15)$$

where  $\boldsymbol{\rho}_0 = \hat{x}x_0 + \hat{y}y_0$  represents the displacement of the obstacle with respect to the beam propagation axis. The Fourier transformations are straightforward and we finally get the following expression for the beam transmitted by the virtual aperture complementary to the obstruction:

$$\psi_A(x, y, z) = \frac{a_R}{z_R} \frac{1}{z - ia_R} \exp\left[i\frac{k}{2}\left(\frac{x^2 + y^2}{z - ia_R}\right)\right], \quad (16)$$

where, for the sake of clarity, we have chosen  $\boldsymbol{\rho}_0 = 0$  and we have defined the modified Rayleigh range  $a_R$  as

$$a_R = \frac{z_R}{1 + \frac{z_R}{ka^2}} \leq z_R. \quad (17)$$

The self-healing mechanism of the Gaussian beam is vividly illustrated in Fig. 2. A close inspection of this figure reveals how the self-reconstruction works. From (17) it follows that  $a_R \leq z_R$ . Therefore, the “virtual” field  $\psi_A(x, y, z)$  transmitted by the complementary aperture spreads in the  $xy$ -plane, while propagating along the  $z$ -axis, much more rapidly than the unperturbed field  $\psi(x, y, z)$  and then for  $z/z_R \gtrsim 2$  the intensity profile of the obstructed beam almost coincides with the profile of the unperturbed one.

The integrals in (12) can be evaluated analytically; the final result is

$$\frac{z_0}{a} = \frac{\pi}{2\theta_0^2} \frac{I_0(1/\theta_0^2) + I_1(1/\theta_0^2)}{\sinh(1/\theta_0^2)}, \quad (18)$$

where  $\theta_0 = 2/(kw_0)$  is the angular spread of the Gaussian beam [27] and  $I_\nu(z)$  is the modified

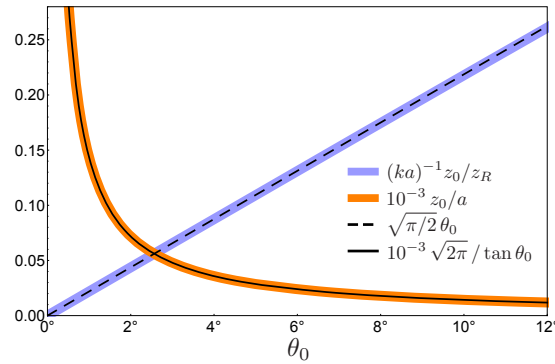


Fig. 3. Minimum reconstruction distance  $z_0/a$  as a function of  $\theta_0$  as well as the paraxial approximation. We also plot  $z_0/z_R$ , which shows a perfect linear behavior. The numerical factor  $10^{-3}$  is introduced to fit both curves in the same scale.

Bessel function of the first kind of order  $\nu$ . In the paraxial regime,  $\theta_0 \ll 1$  and then

$$\frac{z_0}{a} \approx \frac{\sqrt{2\pi}}{\tan \theta_0}, \quad (19)$$

which is consistent with the expected geometrical optics result. A plot of  $z_0/a$  is given in Fig. 3, as well as the paraxial approximation, which works pretty well. Notice that  $z_0$  is larger for smaller  $\theta_0$ , which might appear counterintuitive. The reason is that for smaller  $\theta_0$ ,  $z_R$  becomes larger. To bypass this drawback, we have also plotted  $z_0/z_R$ , which can be easily obtained from (18). For  $\theta_0 \ll 1$ , we get

$$\frac{z_0}{z_R} \approx ka \sqrt{\frac{\pi}{2}} \theta_0. \quad (20)$$

The goodness of this linear approximation can be appreciated in Fig. 3.

## 5. Quantifying self-healing

We still have a conundrum pending from the end of Sec. 2: how is it possible to obtain the simultaneous validity of both (1) and (5)?

Indeed, what one really needs is simply to satisfy (5) on the  $xy$ -plane in the neighborhood of the propagation axis  $z$ . This statement may be formalized as follows. Consider again the obstruction represented in Fig. 1 that occupies the region  $O$  in the  $xy$ -plane. Let  $E$  be an arbitrary area in the  $xy$ -plane *strictly* contained within  $O$ . For example,  $E$  can be the region confined by the inner circle of radius  $b$ , although different symmetries in the problem may dictate different choices. Then, as a necessary condition for self-healing, we require that the amplitude  $\Psi_O(x, y, z)$  of the obstructed beam is proportional to the amplitude  $\Psi(x, y, z)$  of the unperturbed beam *only* within  $E$ ; viz,

$$\Psi_O(x, y, z) \Big|_{(x,y) \in E} \approx \lambda_0 \Psi(x, y, z) \Big|_{(x,y) \in E} \quad \forall z \geq z_0. \quad (21)$$

From a mathematical point of view, (21) makes much more sense than (5). In fact, the field configuration at  $z = 0$  completely determines the field distribution at  $z > 0$ . Then, if at a certain distance  $z$ , (5) were satisfied upon *all* the  $xy$ -plane, then it should be also valid at  $z = 0$ . But the latter statement is clearly false because at  $z = 0$  one has, by definition,  $\Psi_O(x, y, 0) = t_O(x, y) \Psi(x, y, 0) \neq \Psi(x, y, 0)$ . Therefore, the *desideratum* of satisfying both equations (1) and (5) over all the  $xy$ -plane cannot be true.

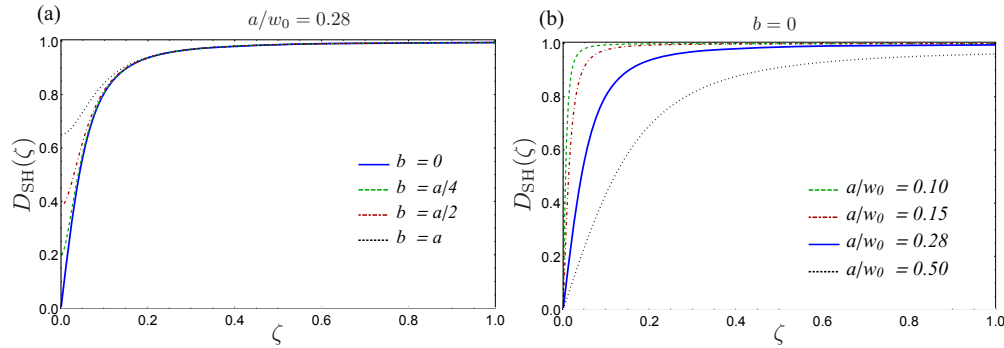


Fig. 4. (a) Plots of the degree of self-healing  $D_{\text{SH}}(z)$  for a Gaussian field of waist  $w_0$  and different radii  $b$  of the integration region  $E$ . The continuous blue line represents the limit value for  $b \rightarrow 0$ . (b) The limit value of  $D_{\text{SH}}(z)$  for  $b \rightarrow 0$ , given in (26), for several values of the width  $a$  of the soft-edge Gaussian obstruction.

To circumvent this difficulty, we first define a scalar product in the space of functions  $L_2(E)$  as

$$\langle f|g \rangle := \int_E f^*(x, y, z)g(x, y, z) dx dy. \quad (22)$$

With this definition, the scalar product  $\langle f|g \rangle$  naturally becomes a function of  $z$ . Of course, the choice of the integration domain  $E$  is partially discretionary (the only constraint is to be entirely contained within  $O$ ). However, it is useful to remind here that the concept of self-healing and minimum reconstruction distance suffer from the same kind of arbitrariness. In other words, since both (1) and (5) are impossible to satisfy over the whole  $xy$ -plane, one is forced to choose *where* these equations should be satisfied. This is because in the total average the field does not heal. This follows from Babinet's principle, the perturbation is somewhere. The beam shape becomes more similar to what it would have been without obstruction because the effect of the obstruction is spread out. To some extent this is the core of any self-healing claim and defining the healing locally at the position of the obstruction bypasses the problem.

The scalar product (22) allows us to introduce in a natural way the corresponding distance  $\mathbb{D}(f, g)$  between two functions in  $L_2(E)$  as  $\mathbb{D}(f, g) = \|f - g\|$ , where  $\|f\| = \langle f|f \rangle^{1/2}$ . This distance somehow quantifies the similarity between the obstructed and the unobstructed field. In quantum information [31] there are many measures of the "closeness" of two (normalized) states we want to compare. Probably, one of the most popular one is the fidelity, a modified version thereof has been proposed in this context by Chu and Wen [32]. However, the standard fidelity fails to furnish a quantitative description of self-healing because it is defined in terms of a scalar product resulting from integration upon the whole  $xy$ -plane and this erases any  $z$ -dependence.

In this paper, we shall use instead the notion of relative distance, which we define as

$$\mathbb{D}_r(\Psi, \Psi_O) = \frac{\|\Psi - \Psi_O\|}{\|\Psi + \Psi_O\|} = \frac{\langle \Psi_A|\Psi_A \rangle^{1/2}}{[\langle \Psi_A|\Psi_A \rangle + 4\langle \Psi|\Psi \rangle - 4\text{Re}\langle \Psi|\Psi_A \rangle]^{1/2}}, \quad (23)$$

where the scalar products are defined as in (22). A direct application of the parallelogram law [33] [ $\|f - g\|^2 + \|f + g\|^2 = 2(\|f\|^2 + \|g\|^2)$ ] immediately confirms that  $0 \leq \mathbb{D}_r^2 \leq 1$ . If  $\Psi_O \approx \lambda_0 \Psi$ , with  $0 \leq \lambda_0 \leq 1$ , then

$$\mathbb{D}_r(\Psi, \Psi_O) \approx \frac{1 - \lambda_0}{1 + \lambda_0}. \quad (24)$$



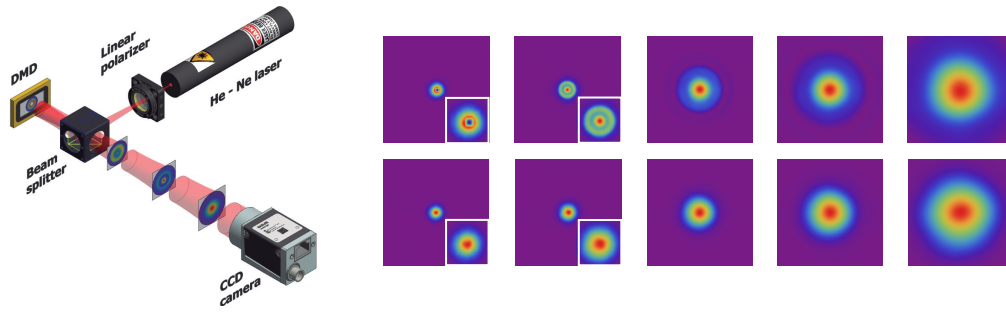


Fig. 5. (Left panel) Experimental setup used to check the self-healing of a fundamental Gaussian beam created by the He-Ne laser. (Right panel) Intensity scans recorded by the CCD camera at increasing distances  $\zeta = 0, 0.5, 1.5, 4$  and  $6.5$  (from left to the right). The beam has a waist  $w_0 = 0.24$  mm, divergence  $\theta_0 = 0.84$  mrad, and Rayleigh range  $z_R = 285$  mm. The upper row corresponds to the obstructed beam (with  $\alpha = 0.206$ ), whereas the lower row is for the unobstructed beam. In the first two scans, the images are very small, so we have included insets (in white frames) with enlarged pictures to better appreciate the patterns.

On that account, we find it convenient to introduce a  $z$ -dependent degree of self-healing:

$$D_{\text{SH}}(z) = \sqrt{1 - \mathbb{D}_r^2(\Psi, \Psi_O)}, \quad (25)$$

and one can check that  $0 \leq D_{\text{SH}}(z) \leq 1$ . We underline that this concept of distance measure has been successfully used in assessing a number of key concepts in quantum optics. In general, a distance measure quantifies the extent to which two physical states behave in the same way. While these distance measures are usually given by certain mathematical expressions, they often possess a simple operational meaning, i.e., they are related to the problem of distinguishing the two states. The notions of nonclassicality [34], entanglement [35], polarization [36], and localization [37], to cite only a few relevant examples, have been systematically formulated within this framework.

For a Gaussian beam, with cylindrical symmetry about the propagation axis  $z$ , we can choose for  $E$  a disk of radius  $b \leq a$ . The function  $D_{\text{SH}}(z)$  can be calculated analytically, although the final expression is complicated and of little use for our purposes. When  $b$  goes to zero, we obtain the asymptotic form

$$D_{\text{SH}}(\zeta) = \zeta \sqrt{\frac{1 - \beta^2}{\beta^2 + \zeta^2}}, \quad (26)$$

where we have used the dimensionless variables

$$\zeta = \frac{z}{z_R}, \quad \alpha = \frac{a}{w_0}, \quad (27)$$

and  $\beta = \alpha^2/(1 + \alpha^2)$ . It is interesting to notice that this function does not depend explicitly on the angular spread  $\theta_0$  of the Gaussian beam.

In Fig. 4(a) we plot  $D_{\text{SH}}(\zeta)$ , for a fixed value of  $\alpha$ , and different radii  $b$  of the integration region  $E$ . When  $b$  increases, the dependence of  $D_{\text{SH}}(\zeta)$  with  $\zeta$  becomes weaker. In Fig. 4(b) we plot the limit form of  $D_{\text{SH}}(\zeta)$ , given in (26), for different values of  $\alpha$ . When  $\alpha$  goes to zero,  $D_{\text{SH}}(\zeta)$  tends to the unity, as expected from physical considerations.

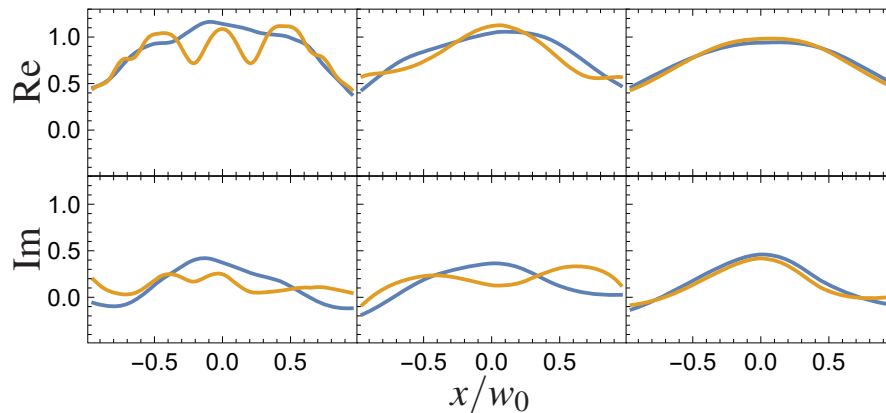


Fig. 6. Real and imaginary parts of the energy-normalized field amplitudes at the positions  $\zeta = 0.05, 0.28,$  and  $0.56$  (from left to right). The obstructed field is represented in orange, while the unobstructed is in blue. The obstruction is characterized by  $\alpha = 0.14$ .

## 6. Experiment

We have checked these predictions in the laboratory. To build up a Gaussian beam with a central obstruction, a He-Ne laser beam (633 nm, Thorlabs) was used. The beam impinges on a digital micromirror device (DMD) chip (Texas Instrument), with square micromirrors of  $7.6 \mu\text{m}$  size each. The obstruction was generated as an off-state region on this chip. A sketch of the setup is presented in Fig. 5. All the previous treatment can be directly applied to this reflection mode.

First, we observed the intensity self-reconstruction of a Gaussian beam of waist  $w_0 = 0.24 \text{ mm}$ , divergence  $\theta_0 = 0.84 \text{ mrad}$ , and Rayleigh range  $z_R = 285 \text{ mm}$ . The beam was propagated a distance  $z = z_R$ , where the half-width is  $w_{z_R} = 0.34 \text{ mm}$ . Then, the DMD is inserted at this position where we generate a centered obstruction of either circular or square shape of half-widths  $a$  of  $0.09 \text{ mm}$ . For both shapes of the obstruction the results are much the same. Then, the intensity scans are captured in several positions by a CCD camera (Basler) with  $5.5 \mu\text{m}$  pixel size. Some of these intensity profiles (for the case of a square obstruction) are depicted in Fig. 5 for different propagating distances from the obstruction.

To experimentally assess the degree of self-healing  $D_{\text{SH}}(\zeta)$  we must be able to measure the

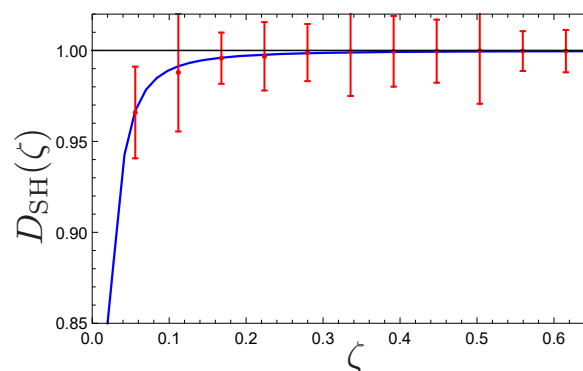


Fig. 7. Experimentally determined degree of self-healing  $D_{\text{SH}}(\zeta)$  obtained from the field measurements shown in Fig. 6. The integration region  $E$  is a dist of radius  $b = a = 0.07 \text{ mm}$ . The error bars represent standard deviations.

whole complex amplitude for both the obstructed and the unobstructed fields, as it is apparent from (23). To facilitate the measurement, a calibrated beam expander was used, so the new waist was  $w_0 = 0.6$  mm and the Rayleigh range  $z_R = 1787$  mm. Then we place alternatively the CCD camera and a Shack-Hartmann wavefront sensor (consisting of a microlens array with  $150 \mu\text{m}$  lens pitch) to the same distance from the DMD and measure the intensity and the wavefront profile of the beam. To increase the wavefront measurement resolution, we used another beam expander coupled directly to the wavefront sensor.

The field complex amplitude was then reconstructed from these measurements that were interpolated to the same resolution. The DMD was positioned now at a distance of 560 mm from the waist with half-width  $w_z = 0.635$  mm. For this measurement, we use the obscuration with  $\alpha = 0.14$ , and detection planes at  $\zeta$  in the range 0.05–0.61. Some of the resulting amplitudes are shown in Fig. 6, where the real and imaginary parts are plotted.

Once the complex amplitudes are experimentally determined, we can compute the degree  $D_{\text{SH}}(\zeta)$ . For this purpose, we take the integration region  $E$  as a disk of radius  $b = a = 0.09$  mm, which is the size of the obstruction. Our experimental results are presented in Fig. 7. For each distance, the measurements have been repeated over 100 times, so we can assign error bars. The agreement with the theory is pretty good.

## 7. Concluding remarks

In summary, we have presented a general theory of the so-called self-healing process occurring in diverse partially obstructed optical beams, whose validity is not limited to diffractionless beams as, e.g., Bessel beams. From a careful analysis of the physical mechanisms involved, we could ascertain the minimum propagation distance from the obstacle after which an optical beam recovers its original intensity profile. Our results, obtained within the framework of wave optics, confirm and extend the traditional ones based on purely geometrical arguments.

We have quantified self-healing as the closeness between the obstructed and unobstructed beams, proposing a suitable measure that has been experimentally tested for Gaussian beams, getting a beautiful agreement with the proposed theory.

## Funding

Technology Agency of the Czech Republic (TE01020229); Grant Agency of the Czech Republic (15-03194S); IGA Palacký University (IGA PrF 2016-005); MINECO (FIS2015-67963-P).

## Acknowledgments

We thank Miguel Alonso for comments that greatly improved the manuscript. G. S. A. thanks the BioPhotonics Initiative of the Texas A&M University.